THE JOURNAL OF PHYSICAL CHEMISTRY C

Article

pubs.acs.org/JPCC

Stabilization of Ultrathin Zinc Oxide Films on Metals: Reconstruction versus Hydroxylation

Bo-Hong Liu, J. Anibal Boscoboinik, Yi Cui, Shamil Shaikhutdinov,* and Hans-Joachim Freund

Abteilung Chemische Physik, Fritz-Haber-Institut der Max-Planck-Gesellschaft, Faradayweg 4-6, 14195 Berlin, Germany

Supporting Information

ABSTRACT: Thin (0001)-oriented films of ZnO on metals may exhibit interlayer relaxations, resulting in the hexagonal boron nitride-like crystal structure. The driving force for such reconstruction is the polar instability of either Zn- or O- terminated surfaces of ZnO(0001). Here, we examined surface hydroxylation as another possible stabilization mechanism. Zinc oxide films grown on Pt(111) were studied by infrared reflection–absorption spectroscopy (IRAS) as a function of film thickness and morphology as imaged by scanning tunneling microscopy. Despite prepared in pure oxygen ambient, the "as grown" films on Pt(111) expose hydroxyl groups. In contrast, the bilayer films on Ag(111) do not exhibit OH species, not even upon dosing of hydrogen or water. The results show that hydrogen may efficiently be provided by a Pt support, even for the multilayer films, via hydrogen dissociation and subsequent diffusion of H atoms through the film. Thermal stability of the OH-terminated surfaces depends on the film thickness, with a monolayer film being the least stable. Removal of OH species from a monolayer film proceeds through water desorption and may be accompanied by hydrogen spillover onto more stable multilayer structures. Stabilization of the polar ZnO surface in the metal-supported films seems to be a delicate balance between interlayer relaxation and hydroxylation and depends on the metal support.

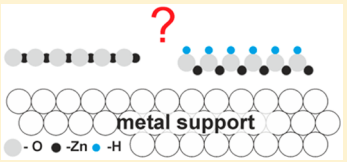

1. INTRODUCTION

Stabilization of polar surfaces in metal oxide systems remains an intriguing fundamental issue in surface science.[1−3] On the basis of studies primarily performed on single crystal surfaces, several possible scenarios are commonly considered: reconstruction via faceting, e.g. the octopolar reconstruction; formation of surface ion vacancies resulting in substoichiometric compositions of the topmost layers; and adsorption of charged adspecies, e.g., by the reaction with ambient gases, in particular of hydrogen and water leading to surface hydroxylation.

In this respect, basal faces of ZnO have been studied quite extensively as classical examples of polar surfaces according to Tasker's classification.[2,4] ZnO crystallizes in hexagonal wurtzite structure, such that the surface perpendicular to the (0001) axis exposes either Zn or O ions in the topmost layer, thus resulting in Zn-terminated, ZnO(0001) and O-terminated, ZnO(000$\bar{1}$) surfaces, respectively, both being polar unstable. For the Zn(0001) surface, scanning tunneling microscopy (STM) and density functional theory (DFT) studies showed that the surface is stabilized by the spontaneous formation of Zn-deficient triangular pits, one layer in depth, with step edges terminated by undercoordinated O atoms.[5] Additional stabilization channel may involve faceting via the formation of regular step arrays.[6] In contrast to the pits formation on ZnO(0001) driven by pure electrostatic considerations, the same arguments did not work for the O-terminated ZnO(000$\bar{1}$) surface. Instead of O-deficient pits, the latter surface showed (n × n)-reconstructed honeycomb-like structures.[7] Another DFT study[8] on various surface reconstructions explained the difference between the two polar surfaces in terms of the different bonding preferences: The Zn atoms are more flexible in their bond formation than O atoms. Such a picture has been recently revisited in combined STM, LEED, and DFT study[9] suggesting that, on both polar surfaces, the undercoordinated Zn ions play a decisive role in shaping the reconstruction structures that cancel the macroscopic dipole moment. Note, however, that the above-mentioned stabilization mechanisms were applied to pristine, H-free surfaces. In fact, the O-terminated surface is known to be very sensitive to the presence of hydrogen and water in the residual gases and hydrogen in bulk interstitials,[4,7,10] resulting in surface hydroxyls via adding H on top of the oxygen ions. Also, an initially Zn-terminated, ZnO(0001) surface may transform into a disordered OH-terminated surface upon water adsorption at room temperature.[11] In fact, many studies point out that the resulted surface structures critically depend on surface preparation.

In addition to ZnO single crystals, thin ZnO films supported on metal surfaces were invoked as model systems well suited for "surface science" tools. Behind the technological applications of ZnO low-dimensional structures,[12] the attention to ultrathin ZnO films has been reinforced since theoretical calculations predicted these films to adopt a hexagonal boron nitride (*h*-BN) like structure, with the O and Zn layers being almost coplanar.[13] These ideas were substantiated by surface X-ray diffraction (SXRD) measurements[14] of ultrathin ZnO films on Ag(111), which revealed strongly reduced interlayer distances for the film thicknesses up to 4 monolayers (ML) (1 ML is referred to Zn−O double layer). To date, ultrathin

Received: February 13, 2015
Revised: March 23, 2015
Published: March 23, 2015

DOI: 10.1021/acs.jpcc.5b01503
J. Phys. Chem. C 2015, 119, 7842−7847

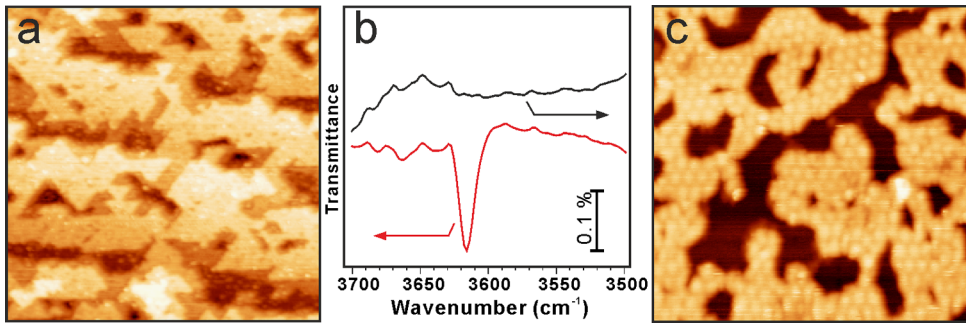

Figure 1. STM images of 5 MLE ZnO films on Pt(111) (a) and 1.5 MLE ZnO films on Ag(111) (c). Sizes are 50 nm × 50 nm; tunneling bias = 1 V, and current = 0.02 nA (a); 1 V and 0.06 nA (c). The ν(OH) region in the corresponding IRA spectra are shown in (b).

ZnO films on Pd(111),[15] Pt(111),[16] Cu(111),[17] Au(111),[18] and brass(111)[19] were fabricated in several research groups. Basically, the *h*-BN-like structure of the resulting films was assumed, although the conclusions were drawn solely on the basis of DFT calculations. Accordingly, such a mechanism is thought to dominate in the case of ultrathin films. On the other hand, very recent SXRD study of the 2−3 ML thick ZnO films grown on Fe(110) revealed bulklike wurtzite structure of the films.[20] The effect was assigned to oxygen "impurity" atoms at the interface between ZnO and Fe(110), leading to a charge redistribution and metallization of the surface layer as judged by DFT, although the calculations were only performed for a small unit cell.

Therefore, the atomic structure of metal-supported ultrathin ZnO films, formed in the course of stabilization of polar surfaces, may even be more complex than considered so far for bulk crystals and additionally depend on the film thickness and the nature of a metal support. Indeed, structural diversity of ZnO monolayer films has been demonstrated for Pd(111)[15] and Pt(111)[16] supports. In contrast, monolayer films were not observed on more noble Ag(111) and Au(111) surfaces, on which the films grow up as bilayer from the onset.[21] In addition, the formation of a Moiré-like coincidence superstructure due to the considerable mismatch between oxide and metal surface lattices may also influence stability of the films.

In order to shed more light on the atomic structure of ultrathin ZnO films, we report here a comparative study of ZnO(0001) films on Pt(111) and Ag(111) using STM and infrared reflection−absorption spectroscopy (IRAS), which is one of the most sensitive and nondamaging tool to identify hydroxyls species. Previously, vibrational spectroscopy has only been applied to ZnO single crystal surfaces[22,23] and nanoparticles,[24,25] which provide a benchmark for the metal-supported thin ZnO films.

2. METHODS AND MATERIALS

The experiments were carried out in two UHV chambers (base pressure 5×10^{-10} mbar). One chamber is equipped with low-energy electron diffraction (LEED, from Omicron), Auger electron spectroscopy (AES), an IRA spectrometer (Bruker IFS 66v), and STM (Omicron). The second UHV chamber is equipped with LEED, AES, STM, and a differentially pumped quadrupole mass spectrometer (HAL 301/3F from Hiden). The same Pt(111) and Ag(111) crystals (from MaTeck GmbH), clamped to an Omicron sample holder, were used in both setups. The sample temperature was measured by a Type K thermocouple spot-welded to the edge of the crystal. A clean Pt(111) surface was obtained by cycles of Ar^+ sputtering and annealing in UHV to 1200 K. Annealing in 10^{-7} mbar of O_2 at ∼700 K was used to remove residual carbon. The Ag(111) surface was cleaned by repeated cycles of Ar^+ sputtering and annealing up to 670 K. The surfaces were carefully cleaned until no contaminations were detected by AES, and STM images showed large, atomically smooth terraces.

Zinc was deposited by heating a Zn rod (1 mm in diameter, 99.99%, Goodfellow) to 480−520 K, passing current through a thoriated tungsten wire wrapped around the rod. The Zn source is shielded by a metal cylinder having a small orifice (∼5 mm in diameter) and placed about 2 cm away from a crystal. The deposition flux was controlled via a Type K thermocouple spot-welded to the edge of the Zn rod.

The films on Pt(111) were prepared by Zn deposition in 10^{-7} mbar of O_2 at room temperature followed by oxidation at 600 K in 10^{-6} mbar of O_2 for 5 min.[16] On Ag(111), films were prepared by the reactive deposition of Zn at room temperature in $\sim 10^{-5}$ mbar of O_2 followed by annealing at 600 K in UHV.[17]

3. RESULTS AND DISCUSSION

Figure 1a shows STM image of relatively "thick" ZnO films, prepared on Pt(111) to about 5 ML in nominal thickness (henceforth used as monolayer equivalent, MLE), as determined by Auger spectroscopy and LEED. The triangular pits formed on the film surface resemble those observed on the Zn-terminated ZnO(0001) single crystal surfaces.[5,11] Solely this similarity would suggest ∼5 MLE thick films to be terminated by Zn. However, the conclusion appears counterintuitive since the clean ZnO(0001)-Zn surfaces are commonly prepared by annealing in UHV at elevated temperatures (∼900 K), whereas our films on Pt(111) were prepared by annealing in 10^{-6} mbar of O_2 at 600 K, thus favoring the O-terminated surfaces.

These "thick" films were further studied by IRAS, which revealed considerable amounts of hydroxyls as evidenced by a sharp peak at 3620 cm^{-1} corresponding to the OH stretching vibrations (Figure 1b). Using an OH-covered silicate film for calibration,[26] the signal intensity corresponds to the OH coverage in the order of 15% with respect to the surface O atoms. The observed frequency (3620 cm^{-1}) is exactly the same as previously obtained by high-resolution electron loss spectroscopy on the OH-covered ZnO$(000\bar{1})$ surface prepared by water adsorption on the (1×3)-reconstructed surface presumably containing oxygen vacancies.[24] (Note, however, that early IRAS studies of the same group on the H(1×1)-ZnO$(000\bar{1})$ surface, although carried out in the other UHV setup, showed the vibrational band at 3572 cm^{-1}.[23]) The presence of OH species in the "as grown" films is a bit

DOI: 10.1021/acs.jpcc.5b01503
J. Phys. Chem. C 2015, 119, 7842−7847

surprising as the films were prepared in the H-free atmosphere and even cooled down to room temperature in oxygen ambient. On the other hand, this finding supports a previously sound view[4,27] (although argued in ref 28) that a defect-free, pure O-terminated ZnO(000$\bar{1}$) surface can hardly be observed in experiment.

In principle, two possible scenarios can be proposed to explain the film hydroxylation. The first one is the reaction of the ZnO films with residual hydrogen containing gases (commonly, H_2 and H_2O) upon staying the "as grown" films in standard UHV conditions (base pressure 5×10^{-10} mbar). The second scenario involves H_2 dissociation on a metal support as previously invoked to explain structural diversity of the monolayer films on Pd(111)[15] and Pt(111).[16] Since Pd and Pt are famous for H_2 dissociation, we have studied, for comparison, ZnO films grown on a Ag(111) substrate, which is essentially inert under UHV-based conditions. Note, however, that for the preparation of well-ordered films on Ag(111) the final annealing at 600 K is performed in UHV.

Figure 1c displays an STM image of the 1.5 MLE ZnO/Ag(111) film, which primarily grows as bilayer (see details in refs 17 and 21). The sample is not fully covered by ZnO that allows better to see effects, if any, of the Ag support on the film hydroxylation. The corresponding IRA spectrum (Figure 1b) does not show any signature of OH species. Moreover, dosing the sample with ~20 L of H_2 or water (D_2O) at 300 K had no effects on the IRA spectra (not shown here). These findings provide strong evidence that (i) the surface of ultrathin ZnO films does not react with water and molecular hydrogen and (ii) hydroxylation observed for ZnO films on Pt(111) is a support-mediated process. Since the ultrathin films on Ag(111) adopt the *h*-BN-like structure,[14] the results also suggest that the depolarization mechanism via an interlayer relaxation prevails over the hydroxylation route in surface stabilization on *pure* ZnO films. One may argue, however, that ~5 MLE thick films on Pt(111) may already transform into the bulklike wurtzite structure, as predicted by DFT,[15] and be, therefore, more reactive to the residual gases. To examine this possibility, in the next set of experiments, we performed IRAS studies of ZnO films on Pt(111) as a function of film thickness. The morphology and film coverage were studied by STM.

Figure 2 depicts IRA spectra obtained for monolayer, bilayer, and ~5 MLE films prepared at the same conditions. Compared to the "thick" films, the bilayer films showed essentially the same density of OH species. In contrast, the monolayer films showed not only a considerably lower integral intensity, but the ν(OH) band apparently splits in two bands, with envelope centered at ~3580 cm^{-1}, i.e., red-shifted by ~40 cm^{-1}, as compared to the bilayer films.

In addition, we examined the thermal stability of OH species. In the first approximation, all films were flashed in UHV to 600 K for comparison. The temperature was chosen to avoid film decomposition that occurs at higher temperatures. Upon anealing, the pressure typically increase up to 2×10^{-9} mbar. The IRAS results (Figure 2) immediately show that the stability is thickness dependent: OH species disappeared from monolayer films but remained intact on 5 MLE films. To monitor this in more detail for the thinnest films, Figure 3b collects a series of IRA spectra obtained upon stepwise heating to elevated temperatures of the sample, exposing both monolayer and bilayer structures (Figure 3a).

The spectrum of the pristine film shows OH features from both, bilayer (at 3620 cm^{-1}) and monolayer (at ~3580 cm^{-1})

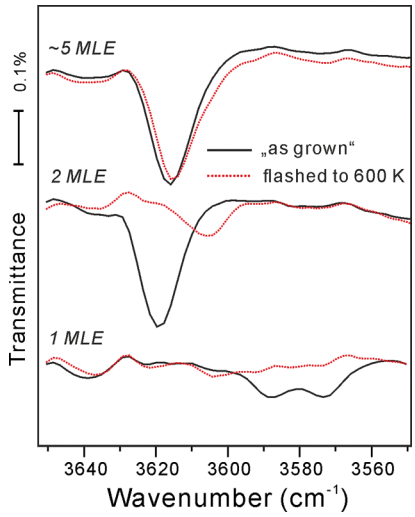

Figure 2. The ν(OH) region in the IRA spectra of ZnO films grown on Pt(111) as a function of the film thickness (in MLE) as indicated. The spectra are normalized to the film coverage, as measured by STM, and are offset for clarity. The spectra after thermal flash to 600 K in UHV are shown as dashed lines. All spectra are recorded at 300 K.

structures. On both surfaces, hydroxyls are fairly stable up to 450 K. After flash to 500 K, OH species on the monolayer disappear with concomitant growth of the signal from bilayer (see Figure 3c) that slightly shifts to 3610 cm^{-1}. This signal enhancement was not observed on a pure bilayer film in similar experiments (see Figure S1 in Supporting Information). It therefore appears that H on the monolayer surface spills over the bilayer islands. Upon further heating, the 3610 cm^{-1} band attenuates, slightly red-shifts, and ultimately disappears at ~750 K. Therefore, the IRAS results show, indeed, that stabilization of ZnO/Pt(111) films via surface hydroxylation depends on the film thickness: The thicker the film, the more stable surface hydroxyls. In principle, this thickness dependence can be rationalized within the "capacitor" model based on pure electrostatic considerations,[3] suggesting that a thicker film possesses a larger net dipole moment to be canceled. The observed trend also correlates with the Zn−O interlayer distance computed by DFT,[15] although for the OH-free films: The thicker the film, the larger the distance, ultimately converging to the situation of wurtzite ZnO.[14] Therefore, "thick" film surfaces may follow, in essence, any of mechanisms proposed for the single crystal surfaces. In contrast, ultrathin (e.g., mono- and bilayer) films may be stabilized by either interlayer relaxation or hydroxylation, if H is provided. The route is essentially governed by the metal support.

To address morphological changes induced by UHV heating in the above experiments, we have performed high-resolution STM study of the films in another UHV setup, additionally equipped with a mass spectrometer for temperature-programmed desorption (TPD) studies. Figure 4 compares STM images of the monolayer film (also exposing few bilayer islands as in Figure 3) before and after thermal flash to 600 K in UHV. Clearly, the annealed film shows a honeycomb-like structure, with a periodicity being exactly the same as the Moiré structure observed in the pristine film. The latter is formed by a coincidence of five ZnO(0001) surface unit cells with six Pt(111) unit cells along the surface lattice directions, i.e., ZnO(0001)-(5×5)/(Pt(111)-(6×6).[16] High-resolution images (inset in Figure 4b) revealed a periodic array of

DOI: 10.1021/acs.jpcc.5b01503
J. Phys. Chem. C 2015, 119, 7842−7847

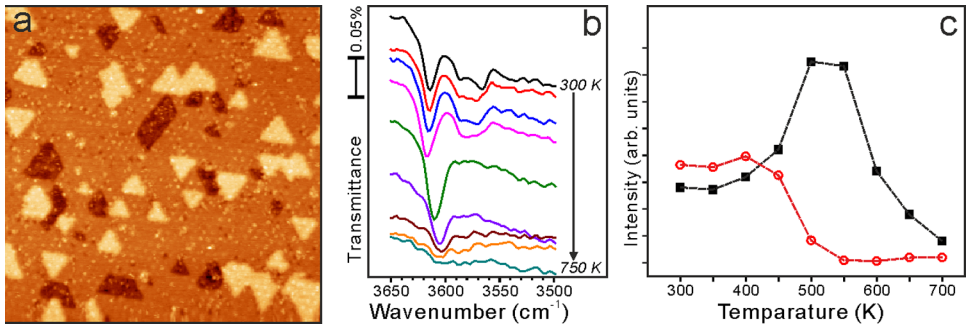

Figure 3. (a) STM image (70 nm × 70 nm, bias = 1 V, and current = 0.1 nA) of "as grown" 1.1 MLE ZnO film on Pt(111), exposing also bilayer islands. (b) ν(OH) region in the IRA spectra measured at 300 K on this film (top spectrum) and after thermal flashes to the temperatures increased stepwise by 50 K up to 750 K. The spectra are offset for clarity. (c) Integral intensity of the 3620 cm^{-1} (in black) and 3580 cm^{-1} (in red) signals as a function of annealing temperature.

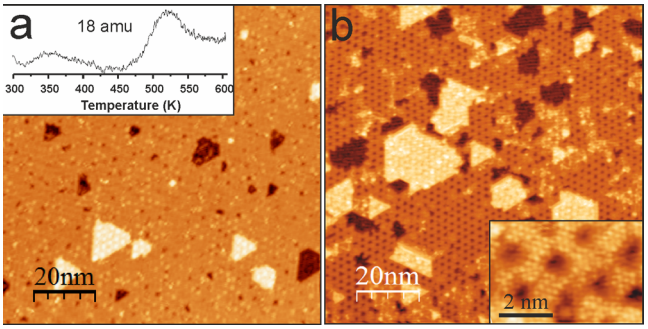

Figure 4. STM images of the 1.2 MLE ZnO film on Pt(111) before (a) and after (b) heating to 600 K in UHV. The inset in (b) shows a high-resolution image of pits in the honeycomb-like structure (tunneling conditions: (a) bias 2 V, current 0.6 nA; (b) 1.5 V, 0.6 nA; (inset) 0.065 V, 0.5 nA). The corresponding TPD spectrum of water (18 amu) signal is shown in the inset in (a). The heating rate is 1 K s^{-1}.

"pits", albeit not all identical, which are about (3 × 3) atomic protrusions in size. Apparently, the double layer thick islands remain to show the Moiré-type surface corrugation as in the pristine film.

From the STM images, it is impossible to say whether the pits are formed by total removal of the Zn and O atoms, or only the O atoms are missing, as the previous DFT calculations suggest the O atoms to constitute the STM contrast of ZnO.[15,18] Comparison of Auger spectra before and after heating did not reveal considerable differences to draw firm conclusions on compositional changes. In addition, neither O_2 (32 amu) nor Zn (66 amu) desorption was detected by a mass spectrometer placed in front of the sample during heating, thus ruling out film sublimation in our conditions.[29] Instead, the TPD spectra showed only water (18 amu) desorption signals: a broad one centered at 350 K and a more pronounced one at 520 K (inset in Figure 4a). Noteworthy, no traces of hydrogen (2 amu) were detected in the spectra (not shown here). Additional STM experiments showed that heating to 450 K does not lead to the pits formation, which must therefore be associated with water desorption at 520 K.

These IRAS and TPD results may readily be explained by recombination of two hydroxyls to form water that desorbs. As the water desorption leaves an oxygen vacancy behind, the observed pits can be assigned to oxygen vacancies. It should also be mentioned that the annealed film shows a considerable number of macroscopic "holes", while the area covered by bilayer islands increases accordingly (compare Figures 4a and 4b). This is indicative for partial dewetting of the film, with the bilayer islands growing at the expense of monolayer structures. In principle, this finding would be consistent with the IRAS results suggesting H spillover from mono- onto bilayer structures, although the precise mechanism remains unclear. In agreement with the IRAS results (Figure 3b), the STM and TPD results show that bilayer structures are, indeed, more stable toward dehydroxylation, which needs much higher temperatures. However, annealing to higher temperatures either in UHV or in oxygen resulted in dewetting and partial decomposition of the film, thus rendering studies on ultrathin films at elevated temperatures nonconclusive.

Interestingly, the (5 × 5) superstructure periodicity in the monolayer film remains after water desorption, indicating that the process is site-dependent within the Moiré unit cell. On the other hand, the honeycomb-like ZnO(0001)-(5 × 5) structure observed here for the annealed monolayer film closely resembles the one recorded (although not atomically resolved) on the ZnO(000$\bar{1}$)-O single crystal surface in UHV at 723 K.[7] Also, water TPD signals (see inset Figure 4a) are similar to those reported for the hydroxylated ZnO(000$\bar{1}$) crystal surfaces,[10] thus suggesting some similarities in their surface structures. On the basis of DFT calculations, the ZnO(000$\bar{1}$)-(5 × 5) structure on a single crystal has been assigned to alternating patches of the regular wurtzite and an unconventional zinc-blende ZnO stacking separated by double-layer holes. Although in our case, the (5 × 5) superstructure seems to be driven by the registry to the metal support underneath and only one layer in thickness, the similarity between the two surfaces is intriguing.

The "as grown" ZnO films on Pt(111) discussed so far were cooled down to room temperature in oxygen ambient, basically to prevent oxide reduction. Since the UHV-annealed monolayer films showed considerable morphological changes (Figure 4), we have also examined a monolayer film prepared at 600 K, with oxygen pumped out simultaneously with cooling. The STM images (Figure 5) revealed another structure, here referred to as "donut"-like, where the protruding Moiré spots exhibit a few missing protrusions in the middle. All atomic protrusions show an ~3.4 Å periodicity, thus assigned to the ZnO(0001) film. (Please note that atomically resolved STM images of a ZnO monolayer on Pd(111) (see Figure 2c in ref 15) and here for Pt(111) differ substantially from those obtained on Ag(111)[14,17] and Au(111),[18] where smooth wavelike surface modulation is observed). On the basis of

DOI: 10.1021/acs.jpcc.5b01503
J. Phys. Chem. C 2015, 119, 7842−7847

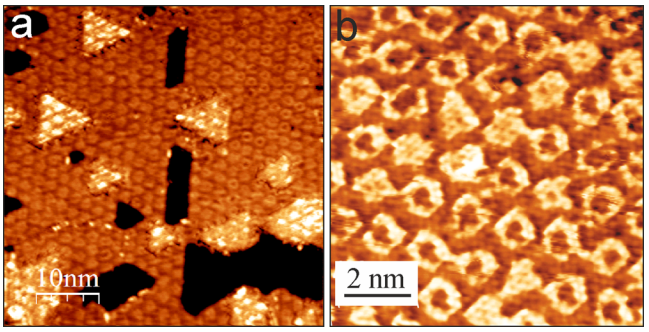

Figure 5. STM images of the 1 MLE ZnO film on Pt(111) prepared by oxidation at 600 K, with oxygen pumped out simultaneously with cooling down to 300 K. Tunneling conditions: bias 0.5 V and current 0.5 nA (a); 0.05 V and 0.5 nA (b).

DFT calculations,[15,18] we have tentatively assigned the missing protrusions to O vacancies which are formed in vacuum in the first moments of cooling while the sample was still at high temperatures. Obviously, the final structures, imaged in Figures 4 and 5, must not necessarily be the same, as they may depend on the "initial" state and also be kinetically limited, thus depending on the cooling (heating) rate. Nonetheless, the mechanism for oxygen vacancies formation on ZnO monolayer in both preparations seems to be similar. Note again that, for both surfaces, the missing protrusions in STM images are distributed not randomly, but at the specific sites within the Moiré unit cell. It, therefore, appears that the oxygen vacancy formation depends on the registry between the ZnO monolayer and the Pt(111) surface.

The precise mechanism of Pt-mediated surface hydroxylation of the ZnO films remains unclear. While for the monolayer films one could envision H spillover from Pt on top of the ZnO monolayer film, for the multilayer films, the mechanism must involve H diffusion through the film to segregate at the surface as hydroxyls. In principle, the DFT-computed distances between a ZnO layer in a *h*-BN-structure and a metal surface (>2.65 Å)[18,30,31] allow hydrogen atoms to intercalate the interface and then migrate into the film. Recently, hydrogen transport through ZnO films on Ag(111) was addressed by DFT.[30] Multicenter bond formation is observed to significantly assist the transport of H adatoms through the ZnO sheet toward metal support. In our case, one has to consider the reverse process, i.e., from the metal support to the ZnO surface.

It is noteworthy that, among ultrathin oxide films of 3d transition metals grown on (111) metal supports, ZnO seems to be the only example of almost a coplanar structure of the film, with the rumpling (i.e., the distance between cation and oxygen layers) of about 0.1 Å. For comparison, for the well-studied FeO(111) films on Pt(111), the rumpling is 0.66 Å,[32] although in both cases the distances are strongly reduced as compared to those in the bulk, i.e., 1.3 and 0.63 Å in FeO (rocksalt) and ZnO (wurtzite), respectively. Electron transfer from FeO, having the lower work function than of Pt(111), drives the positively charged Fe ions to be at the interface.[32] If the same arguments hold true for the ZnO(0001) films, this would favor the O-termination, which could be stabilized either via the interlayer relaxation into the *h*-BN structure as observed for Ag(111)-supported films or the surface hydroxylation as observed on ZnO(000$\bar{1}$) single crystals. Certainly, the second mechanism dominates on Pt(111) which provides atomic hydrogen while Ag does not. On the other hand, the same Pt-mediation scenario could, in principle, be applied for the FeO(111) films as well. However, neither "as grown" nor water-exposed FeO(111) films on Pt(111) are hydroxylated.[33,34] To explain the difference, we recall that interstitial hydrogen is very common for ZnO[10] and not for iron oxides. Therefore, the high affinity of ZnO for hydrogen could be another factor that favors surface hydroxylation observed in "as grown" ultrathin films on Pt(111). Further, both experimental and theoretical studies remain to be performed to more deeply understand the Pt (and Pd)-mediated surface hydroxylation of ZnO thin films.

4. CONCLUSIONS

Based primarily on DFT-derived theoretical grounds, thin films of ZnO are thought to exhibit interlayer relaxations, resulting in the hexagonal boron nitride-like crystal structure, driven by polar instability of either Zn- or O-terminated surfaces of ZnO(0001). In order to shed light on stabilization mechanisms for such films, in particular through surface hydroxylation, ultrathin ZnO films grown on Pt(111) were studied here by IRAS and STM as a function of film thickness. Despite being prepared in pure oxygen ambient, the "as grown" ZnO films on Pt(111) all expose hydroxyl groups. Thermal stability of the OH-terminated surfaces depends on the film thickness, with a monolayer film being the least stable. Removal of OH species from a monolayer film proceeds through water desorption and may be accompanied by hydrogen spillover onto more stable multilayer structures. In contrast, the ultrathin films on Ag(111) do not exhibit OH species, not even upon dosing of hydrogen or water. Stabilization of the polar ZnO surface in the metal-supported films is, therefore, a delicate balance between interlayer relaxation and hydroxylation. Apparently, the relaxation dominates in Ag(111)-supported films, while the second mechanism dominates for a Pt(111) support which is able to provide atomic hydrogen. In addition, the high affinity of ZnO for hydrogen seems to be another factor that favors surface hydroxylation observed in thin films grown on Pt(111).

The observation of surface hydroxyls on the "as prepared" ZnO/Pt films can be traced back to other prior studies where water/hydroxyl's have been missed/ignored erroneously. In particular, thin NiO(111) films grown on Ni(111) were shown to be covered by hydroxyls as prepared. Upon heat treatment, the hydroxyl groups are removed, and the surface reconstructs into the octopolar-type (2 × 2) structure.[35] Also for MgO (111), single crystal surfaces showed significant coverages of hydroxyl terminations, even after UHV annealing.[36]

Finally, we mention that previous angle-resolved X-ray photoelectron spectroscopy studies of ZnO crystals indicated good possibilities for using this technique for polarity determination of wurtzite type crystal surfaces.[37,38] Also, this issue could be addressed using adsorption of some simple probe molecules.[38] These works are currently in progress.

■ ASSOCIATED CONTENT

Supporting Information

IRA spectra as a function of annealing temperature observed for a pure bilayer ZnO film. This material is available free of charge via the Internet at http://pubs.acs.org.

■ AUTHOR INFORMATION

Corresponding Author

*Phone +49 30 84134114; e-mail shaikhutdinov@fhi-berlin.mpg.de (S.S.).

DOI: 10.1021/acs.jpcc.5b01503
J. Phys. Chem. C 2015, 119, 7842−7847

Notes

The authors declare no competing financial interest.

■ ACKNOWLEDGMENTS

B.H.L. thanks the International Max Planck Research School "Functional interfaces in physics and chemistry" for a fellowship. Y.C. and J.A.B. acknowledge Alexander von Humboldt Foundation for the fellowships. The work has been supported by Deutsche Forschungsgemeinschaft through the collaborative research center SFB 1109 and by COST Action CM1104.

■ REFERENCES

(1) Noguera, C. Polar Oxide Surfaces. *J. Phys.: Condens. Matter* **2000**, *12*, R367.
(2) Goniakowski, J.; Finocchi, F.; Noguera, C. Polarity of Oxide Surfaces and Nanostructures. *Rep. Prog. Phys.* **2008**, *71*, 016501.
(3) Noguera, C.; Goniakowski, J. Polarity in Oxide Nano-objects. *Chem. Rev.* **2012**, *113*, 4073−4105.
(4) Wöll, C. The Chemistry and Physics of Zinc Oxide urfaces. *Prog. Surf. Sci.* **2007**, *82*, 55−120.
(5) Dulub, O.; Diebold, U.; Kresse, G. Novel Stabilization Mechanism on Polar Surfaces: ZnO(0001)-Zn. *Phys. Rev. Lett.* **2003**, *90*, 016102.
(6) Ostendorf, F.; Torbrügge, S.; Reichling, M. Atomic Scale Evidence for Faceting Stabilization of a Polar Oxide Surface. *Phys. Rev. B* **2008**, *77*, 041405.
(7) Lauritsen, J. V.; Porsgaard, S.; Rasmussen, M. K.; Jensen, M. C. R.; Bechstein, R.; Meinander, K.; Clausen, B. S.; Helveg, S.; Wahl, R.; Kresse, G.; Besenbacher, F. Stabilization Principles for Polar Surfaces of ZnO. *ACS Nano* **2011**, *5*, 5987−5994.
(8) Wahl, R.; Lauritsen, J. V.; Besenbacher, F.; Kresse, G. Stabilization Mechanism for the Polar ZnO(0001)-O surface. *Phys. Rev. B* **2013**, *87*, 085313.
(9) Xu, H.; Dong, L.; Shi, X. Q.; Van Hove, M. A.; Ho, W. K.; Lin, N.; Wu, H. S.; Tong, S. Y. Stabilizing Forces Acting on ZnO Polar Surfaces: STM, LEED, and DFT. *Phys. Rev. B* **2014**, *89*, 235403.
(10) Qiu, H.; Meyer, B.; Wang, Y.; Wöll, C. Ionization Energies of Shallow Donor States in ZnO Created by Reversible Formation and Depletion of H Interstitials. *Phys. Rev. Lett.* **2008**, *101*, 236401.
(11) Önsten, A.; Stoltz, D.; Palmgren, P.; Yu, S.; Göthelid, M.; Karlsson, U. O. Water Adsorption on ZnO(0001): Transition from Triangular Surface Structures to a Disordered Hydroxyl Terminated phase. *J. Phys. Chem. C* **2010**, *114*, 11157−11161.
(12) Wang, Z. L. Splendid One-Dimensional Nanostructures of Zinc Oxide: A New Nanomaterial Family for Nanotechnology. *ACS Nano* **2008**, *2*, 1987−1992.
(13) Claeyssens, F.; Freeman, C. L.; Allan, N. L.; Sun, Y.; Ashfold, M. N. R.; Harding, J. H. Growth of ZnO Thin Films - Experiment and Theory. *J. Mater. Chem.* **2005**, *15*, 139−148.
(14) Tusche, C.; Meyerheim, H. L.; Kirschner, J. Observation of Depolarized ZnO(0001) Monolayers: Formation of Unreconstructed Planar Sheets. *Phys. Rev. Lett.* **2007**, *99*, 026102.
(15) Weirum, G.; Barcaro, G.; Fortunelli, A.; Weber, F.; Schennach, R.; Surnev, S.; Netzer, F. P. Growth and Surface Structure of Zinc Oxide Layers on a Pd(111) Surface. *J. Phys. Chem. C* **2010**, *114*, 15432−15439.
(16) Liu, B.-H.; McBriarty, M. E.; Bedzyk, M. J.; Shaikhutdinov, S.; Freund, H.-J. Structural Transformations of Zinc Oxide Layers on Pt(111). *J. Phys. Chem. C* **2014**, *118*, 28725−28729.
(17) Pan, Q.; Liu, B. H.; McBriarty, M. E.; Martynova, Y.; Groot, I. M. N.; Wang, S.; Bedzyk, M. J.; Shaikhutdinov, S.; Freund, H. J. Reactivity of Ultra-Thin ZnO Films Supported by Ag(111) and Cu(111): A Comparison to ZnO/Pt(111). *Catal. Lett.* **2014**, *144*, 648−655.
(18) Deng, X.; Yao, K.; Sun, K.; Li, W.-X.; Lee, J.; Matranga, C. Growth of Single- and Bilayer ZnO on Au(111) and Interaction with Copper. *J. Phys. Chem. C* **2013**, *117*, 11211−11218.
(19) Schott, V.; Oberhofer, H.; Birkner, A.; Xu, M.; Wang, Y.; Muhler, M.; Reuter, K.; Wöll, C. Chemical Activity of Thin Oxide Layers: Strong Interactions with the Support Yield a New Thin-Film Phase of ZnO. *Angew. Chem., Int. Ed.* **2013**, *52*, 11925−11929.
(20) Meyerheim, H. L.; Ernst, A.; Mohseni, K.; Tusche, C.; Adeagbo, W. A.; Maznichenko, I. V.; Hergert, W.; Castro, G. R.; Rubio-Zuazo, J.; Morgante, A.; Jedrecy, N.; Mertig, I.; Kirschner, J. Wurtzite Structure in Ultrathin ZnO films on Fe(110): Surface X-ray Diffraction and Ab initio Calculations. *Phys. Rev. B* **2014**, *90*, 085423.
(21) Shiotari, A.; Liu, B. H.; Jaekel, S.; Grill, L.; Shaikhutdinov, S.; Freund, H.-J.; Wolf, M.; Kumagai, T. Local Characterization of Ultrathin ZnO Layers on Ag(111) by Scanning Tunneling Microscopy and Atomic Force Microscopy. *J. Phys. Chem. C* **2014**, *118*, 27428−27435.
(22) Wang, Y. High Resolution Electron Energy Loss Spectroscopy on Perfect and Defective Oxide Surfaces. *Z. Phys. Chem.* **2008**, *222*, 927.
(23) Schiek, M.; Al-Shamery, K.; Kunat, M.; Traeger, F.; Woll, C. Water Adsorption on the Hydroxylated H-(1 × 1) O-ZnO(0001) Surface. *Phys. Chem. Chem. Phys.* **2006**, *8*, 1505−1512.
(24) Noei, H.; Qiu, H.; Wang, Y.; Loffler, E.; Woll, C.; Muhler, M. The Identification of Hydroxyl Groups on ZnO Nanoparticles by Infrared Spectroscopy. *Phys. Chem. Chem. Phys.* **2008**, *10*, 7092−7097.
(25) Viñes, F.; Iglesias-Juez, A.; Illas, F.; Fernández-García, M. Hydroxyl Identification on ZnO by Infrared Spectroscopies: Theory and Experiments. *J. Phys. Chem. C* **2013**, *118*, 1492−1505.
(26) Yang, B.; Shaikhutdinov, S.; Freund, H.-J. Tuning Spatial Distribution of Surface Hydroxyls on a Metal-Supported Single-Layer Silica. *J. Phys. Chem. Lett.* **2014**, *5*, 1701−1704.
(27) Meyer, B. First-Principles Study of the Polar O-Terminated ZnO Surface in Thermodynamic Equilibrium with Oxygen and Hydrogen. *Phys. Rev. B* **2004**, *69*, 045416.
(28) Lindsay, R.; Muryn, C. A.; Michelangeli, E.; Thornton, G. ZnO−O Surface Structure: Hydrogen-free (1 × 1) Termination. *Surf. Sci.* **2004**, *565*, L283−L287.
(29) Kohl, D.; Henzler, M.; Heiland, G. Low Temperature Sublimation Processes from Clean Cleaved Polar Surfaces of Zinc Oxide Crystals during First Heating. *Surf. Sci.* **1974**, *41*, 403−411.
(30) Demiroglu, I.; Stradi, D.; Illas, F.; Bromley, S. T. A Theoretical Study of a ZnO Graphene Analogue: Adsorption on Ag(111) and Hydrogen Transport. *J. Phys.: Condens. Matter* **2011**, *23*, 334215.
(31) Barcaro, G.; Thomas, I. O.; Fortunelli, A. Validation of Ddensity-Functional Versus Density-Functional+U Approaches for Oxide Ultrathin Films. *J. Chem. Phys.* **2010**, *132*, 124703.
(32) Goniakowski, J.; Noguera, C.; Giordano, L.; Pacchioni, G. Adsorption of Metal Adatoms on FeO(111) and MgO(111) Monolayers: Effects of Charge State of Adsorbate on Rumpling of Supported Oxide Film. *Phys. Rev. B* **2009**, *80*, 125403.
(33) Joseph, Y.; Ranke, W.; Weiss, W. Water on FeO(111) and Fe_3O_4(111): Adsorption Behavior on Different Surface Terminations. *J. Phys. Chem. B* **2000**, *104*, 3224−3236.
(34) Leist, U.; Ranke, W.; Al-Shamery, K. Water Adsorption and Growth of Ice on Epitaxial Fe_3O_4(111), FeO(111) and Fe_2O_3(biphase). *Phys. Chem. Chem. Phys.* **2003**, *5*, 2435−2441.
(35) Rohr, F.; Wirth, K.; Libuda, J.; Cappus, D.; Bäumer, M.; Freund, H. J. Hydroxyl Driven Reconstruction of the Polar NiO(111) surface. *Surf. Sci.* **1994**, *315*, L977−L982.
(36) Ciston, J.; Subramanian, A.; Marks, L. D. Water-Driven Structural Evolution of the Polar MgO(111) Surface: An Integrated Experimental and Theoretical Approach. *Phys. Rev. B* **2009**, *79*, 085421.
(37) Williams, J. R.; Kobata, M.; Pis, I.; Ikenaga, E.; Sugiyama, T.; Kobayashi, K.; Ohashi, N. Polarity Determination of Wurtzite-type Crystals Using Hard X-ray Photoelectron Diffraction. *Surf. Sci.* **2011**, *605*, 1336−1340.
(38) Yoshihara, J.; Campbell, J. M.; Campbell, C. T. Cu Films on a Zn-Terminated ZnO(0001) Surface: Structure and Electronic Properties. *Surf. Sci.* **1998**, *406*, 235−245.

DOI: 10.1021/acs.jpcc.5b01503
J. Phys. Chem. C 2015, 119, 7842−7847